

# Effects of Wall Impedance on Transmission and Attenuation of Higher-order Modes in Vocal-tract Model

Kunitoshi Motoki<sup>1</sup>

<sup>1</sup>Department of Electronics and Information Engineering, Hokkai-Gakuen University, Japan

motoki@eli.hokkai-s-u.ac.jp

## Abstract

This paper presents the effects of a wall impedance on the propagation of higher-order modes in a three-dimensional vocal-tract model. This model is constructed using an asymmetrically connected structure of rectangular acoustic tubes, and can parametrically represent acoustic characteristics in higher frequencies where the assumption of the plane wave propagation does not hold. The propagation constants of the higher-order modes are calculated taking account of the wall impedance. The resonance characteristics of the vocal-tract model are evaluated based on the transfer impedance between an input volume velocity and an output sound-pressure.

**Index Terms:** vocal-tract model, higher-order modes, wall impedance

## 1. Introduction

The acoustic analysis of three-dimensional vocal-tract models in higher frequencies has been performed by many researchers based on the geometrical data obtained by magnetic resonance imaging. A finite element method (FEM) is a standard numerical simulation technique for investigating the effects of the fine three-dimensional structure of the vocal-tract such as small dips or branches [1, 2]. However, FEM requires a large amount of time not only for the computation itself, but also for the creation of finite element meshes.

On the other hand, a parametric method to compute the acoustic characteristics in higher frequencies, where the assumption of plane wave propagation does not hold, has been developed by using higher-order modes [3, 4]. The vocal-tract is approximated by a cascaded structure of rectangular acoustic tubes. Although the performance in representing the detailed structure of the vocal-tract is not high, this method can represent the effects of the transverse dimension of the vocal-tract in higher frequencies, and has an advantage of fast computation since this method can be regarded as an extension of a well-known one-dimensional vocal-tract model.

Even though the radiation factor is taken into account, the resonance characteristics of three-dimensional vocal-tract model with internal loss-less condition generally contain many sharp peaks and zeros in higher frequencies above the frequency limit of plane wave propagation.

In this paper a wall impedance is introduced in the computation of the propagation constant of the higher-order modes, and the transfer characteristics of the proposed model are evaluated for different values of the wall impedance. Results show an increase of bandwidth and a slight upward shift of peaks especially in lower frequencies, as already suggested by one-dimensional model. It is also shown that the sharp peaks in higher frequencies are less sensitive to the values of the

wall impedance even though the attenuation of the higher-order modes is larger than that of a plane wave.

## 2. Acoustic model with higher-order modes

### 2.1. Model description

A cascaded structure of rectangular acoustic tubes, connected asymmetrically with respect to their axes as illustrated in figure 1, is introduced as an approximation of the vocal tract geometry. The width, height, length and the position of the axis of each tube can be specified independently. A sound source can be specified as an arbitrary vibrating surface on the entrance of the first section. The last section corresponding to the mouth is open to a free space. The radiation of sound is taken into account. The wall of each rectangular tube has yielding properties that can be specified by the wall impedance.

### 2.2. Propagation constant of higher-order mode

The sound-pressure  $p(x, y, z)$ ,  $z$  being the direction of the tube axis, and the particle velocity  $\mathbf{v}(x, y, z)$  can be expressed as,

$$p(x, y, z) = j\omega\rho\phi(x, y, z) \quad (1)$$

$$\mathbf{v}(x, y, z) = -\nabla\phi(x, y, z) \quad (2)$$

where  $\omega$  and  $\rho$  are angular frequency and air density.  $\phi(x, y, z)$  is a velocity potential satisfying the Helmholtz equation.

$$\nabla^2\phi(x, y, z) + k^2\phi(x, y, z) = 0 \quad (3)$$

$k = \omega/c$ ,  $c$ : sound speed, is a wave number. The three-dimensional acoustic field in each tube can be represented in infinite series of higher-order modes as,

$$\phi(x, y, z) = \sum_{m,n=0}^{\infty} (a_{mn}e^{-\gamma_{z,mn}z} + b_{mn}e^{\gamma_{z,mn}z})\psi_{mn}(x, y) \quad (4)$$

where  $m$  and  $n$  stand for the numbers of the higher-order modes in  $x$  and  $y$  directions,  $a_{mn}$  and  $b_{mn}$  are constant determined from the geometry of adjacent tubes.  $\gamma_{z,mn}$  and  $\psi_{mn}(x, y)$  are the propagation constant and normal function (eigen function), respectively.  $\psi_{mn}(x, y)$  can be written as,

$$\psi_{mn}(x, y) = H_{cs}(m, \gamma_{x,m}x) H_{cs}(n, \gamma_{y,n}y) \quad (5)$$

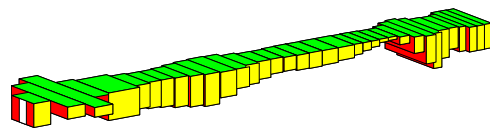


Figure 1: Cascaded structure of rectangular tubes.

where  $H_{cs}(q, \theta)$  is defined as follows.

$$H_{cs}(q, \theta) = \begin{cases} \cosh(\theta) & q = 0, 2, 4, \dots \\ \sinh(\theta) & q = 1, 3, 5, \dots \end{cases} \quad (6)$$

$\gamma_{x,m}$ ,  $\gamma_{y,n}$  and  $\gamma_{z,mn}$  are required to satisfy the following relation.

$$\gamma_{x,m}^2 + \gamma_{y,n}^2 + \gamma_{z,mn}^2 + k^2 = 0 \quad (7)$$

$\gamma_{z,mn}$  is to be determined by specifying the boundary condition on the wall. A wall impedance  $Z_w$  is defined as the ratio of the sound pressure  $p$  to the particle velocity component  $v_n$  normal to the wall surface. By applying the theory of lined duct [5, 6], wall boundary condition can be represented separately for even and odd modes in  $x$ -direction.

#### Even modes

$$\frac{\partial p}{\partial x} \Big|_{x=0} = 0 \quad (8)$$

$$Z_w = \frac{p}{\pm v_x} \Big|_{x=\pm L_x/2} = -j \frac{\omega \rho}{\gamma_{x,m}} \coth\left(\gamma_{x,m} \frac{L_x}{2}\right)$$

#### Odd modes

$$p \Big|_{x=0} = 0 \quad (9)$$

$$Z_w = \frac{p}{\pm v_x} \Big|_{x=\pm L_x/2} = -j \frac{\omega \rho}{\gamma_{x,m}} \tanh\left(\gamma_{x,m} \frac{L_x}{2}\right)$$

$L_x$  is the sectional dimension of the rectangular tube in  $x$ -direction as illustrated in figure 2. From eqs (8) and (9),  $\gamma_{x,m}$  is obtained as,

$$\gamma_{x,m} = \begin{cases} e^{j\frac{3}{4}\pi} \sqrt{\frac{2k\bar{Y}}{L_x}} & m = 0 \\ \frac{j\pi}{L_x} \left(m + j\frac{2kL_x\bar{Y}}{m\pi^2}\right) & m = 1, 2, 3, \dots \end{cases} \quad (10)$$

where  $\bar{Y}$  is normalized wall admittance defined by  $\bar{Y} = \rho c / Z_w$ , and  $|\bar{Y}| \ll 1$  is assumed. Similar relations can be written in  $y$ -direction.

$$\gamma_{y,n} = \begin{cases} e^{j\frac{3}{4}\pi} \sqrt{\frac{2k\bar{Y}}{L_y}} & n = 0 \\ \frac{j\pi}{L_y} \left(n + j\frac{2kL_y\bar{Y}}{n\pi^2}\right) & n = 1, 2, 3, \dots \end{cases} \quad (11)$$

Then  $\gamma_{z,mn}$ 's, propagation constant of mode  $(m, n)$  in  $z$ -direction, are calculated as follows.

$$\gamma_{z,mn} = \alpha_{z,mn} + j\beta_{z,mn} = \sqrt{-(\gamma_{x,m}^2 + \gamma_{y,n}^2 + k^2)} \quad (12)$$

$\alpha_{z,mn}$  and  $\beta_{z,mn}$  are attenuation and phase constants, respectively. A mode  $(0,0)$  represents plane wave, others are higher-order modes. The rigid wall condition corresponds to  $|\bar{Y}| = 0$ , and  $\gamma_{z,mn}$  is reduced to

$$\gamma_{z,mn} = \sqrt{\left(\frac{m\pi}{L_x}\right)^2 + \left(\frac{n\pi}{L_y}\right)^2 - k^2}. \quad (13)$$

In this condition, the cut-off frequency  $f_{c,mn}$  of mode  $(m, n)$  is calculated as a frequency where  $\gamma_{z,mn} = 0$ .

$$f_{c,mn} = \frac{c}{2\pi} \sqrt{\left(\frac{m\pi}{L_x}\right)^2 + \left(\frac{n\pi}{L_y}\right)^2} \quad (14)$$

The higher-order modes are propagative above  $f_{c,mn}$ , and are evanescent,  $\beta_{z,mn} = 0$ , below  $f_{c,mn}$ . The evanescent modes are mainly excited at the part of discontinuity in the shape, and

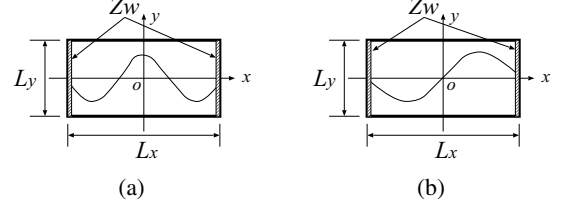


Figure 2: Example of sound-pressure distributions, (a) even mode (b) odd mode.

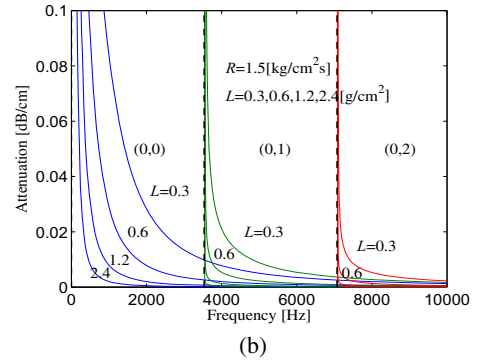
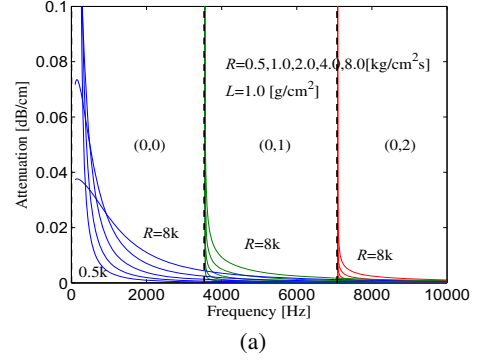


Figure 3: Attenuation of modes  $(0,0)$ ,  $(0,1)$  and  $(0,2)$ , tube size:  $L_x = 1.5$ [cm],  $L_y = 5.0$ [cm]. Vertical dashed lines indicate cut-off frequencies for rigid wall condition,  $f_{c,01} = 3539$ [Hz],  $f_{c,02} = 2f_{c,01}$ . Variation with respect to (a)  $R$  and (b)  $L$ .

are localized in the vicinity of the excitation part. In order to represent the variation of the acoustic field in the vicinity of the part with rapid change in sectional shape, several higher-order modes, not only propagative modes but also evanescent modes, need to be considered. In the case of soft wall condition,  $\bar{Y} \neq 0$ , the exact cut-off frequency can not be obtained as  $\gamma_{z,mn}$  does not become 0. However, as  $\bar{Y}$  is small, it is presumably assumed that the resonances due to the higher-order modes will appear in frequencies above  $f_{c,mn}$ . If no higher-order mode is considered, *i.e.* plane waves only, this model is identical to the ordinary one-dimensional model of speech production.

## 3. Computational results

### 3.1. Attenuation and phase constants

As the wall impedance of the vocal-tract is an important physical parameter, its value has been directly measured or indirectly estimated using different methodologies. The measured values

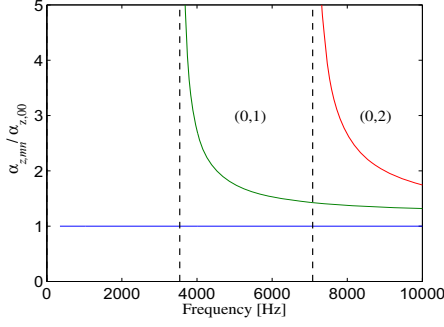


Figure 4: The ratio of the attenuation constants of modes (0,1) and (0,2) to (0,0).  $Z_w = 1900 + j\omega 0.3[\text{g}/(\text{cm}^2)\text{s}]$

showed a relatively wide variety of range depending on methods and position of the human body [7–12]. The attenuation constant  $\alpha_{z,mn}$  and phase constant  $\beta_{z,mn}$  are computed with changing the resistive term  $R$  and inertia term  $L$  of the wall impedance  $Z_w = R + j(\omega L - K/\omega)$ . A stiffness term  $K$  was ignored in this computation.

Figure 3 shows the attenuation of modes (0,0),(0,1) and (0,2) per unit length,  $20 \log e^{\alpha_{z,mn}}$ , for the tube dimension of  $L_x = 1.5[\text{cm}]$ ,  $L_y = 5.0[\text{cm}]$ . Vertical dashed lines indicate cut-off frequencies  $f_{c,mn}$  for rigid wall condition.  $L$  has relatively large influence than the variation in  $R$  on both plane wave and higher-order modes. The attenuation in the vicinity of the cut-off frequencies is especially large. Figure 4 shows the ratio of  $\alpha_{z,mn}$  to  $\alpha_{z,00}$ . The attenuation of higher-order modes is always larger than that of the plane wave.

Figure 5 shows the difference of the phase constant relative to that of the rigid wall condition. For mode (0,0), difference rate is large in the frequency range below 2 kHz, which means that if a resonance frequency appears in this range, the resonance frequency will shift upward compared to the case of the rigid wall. For higher-order modes, upward shift can be possibly caused when the peak frequency is very close to the cut-off frequency.

### 3.2. Transfer characteristics

Transfer characteristics of the model are evaluated in terms of the transfer impedance  $Z$ , the ratio of the sound-pressure  $p_r$  at a distant point to the given source volume velocity  $U_G$ . At the distant point,  $p_r$  can be assumed to be proportional to the root of the total power  $W_C$  radiated from the model.

$$Z = \frac{p_r}{U_G} = K_z \frac{\sqrt{W_C}}{U_G}, K_z : \text{const.} \quad (15)$$

$W_C$  can be evaluated at the open end of the tube using the parametric representation of higher-order modes [3].

#### 3.2.1. Uniform rectangular tube

The transfer characteristics of a uniform rectangular tube (total length  $L_z = 17[\text{cm}]$ ) are shown in figure 6 changing the values of inertia term  $L$ . A rigid wall condition is also shown in the top for the purpose of comparison. The lower peaks, especially below in 1 kHz, are largely influenced with respect to the bandwidth by the variation of  $L$ . Compared with the rigid wall condition, a small upward shift of peak frequencies is also seen. Some sharp peaks above 3.5 kHz are the resonance of the

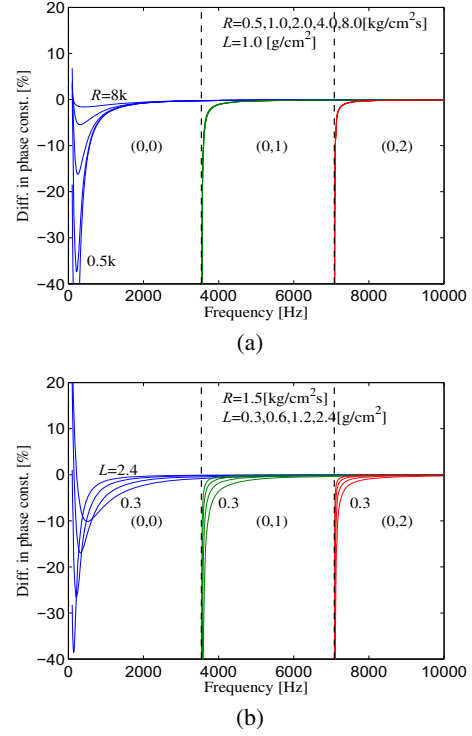


Figure 5: Difference of the phase constant relative to that of the rigid wall condition.  $(\beta_{z,mn}[\text{soft}] - \beta_{z,mn}[\text{rigid}])/\beta_{z,mn}[\text{rigid}] \times 100 \%$ . Variation with respect to (a)  $R$  and (b)  $L$ .

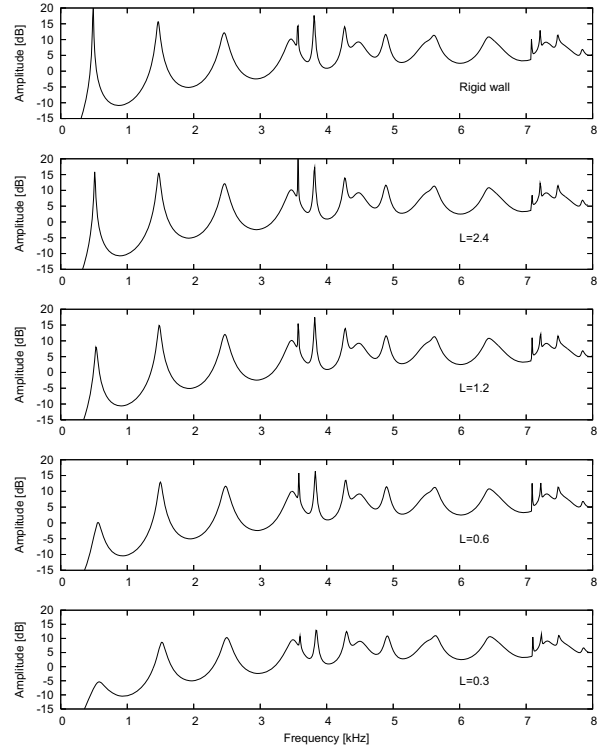


Figure 6: Transfer characteristics of a uniform rectangular tube of size:  $L_x = 1.5[\text{cm}]$ ,  $L_y = 5.0[\text{cm}]$ ,  $L_z = 17[\text{cm}]$ .  $Z_w = R + j\omega L$ ,  $R = 1500[\text{g}/(\text{cm}^2 \cdot \text{s})]$ . From top to bottom, rigid wall,  $L = 2.4, 1.2, 0.6, 0.3[\text{g}/\text{cm}^2]$ .

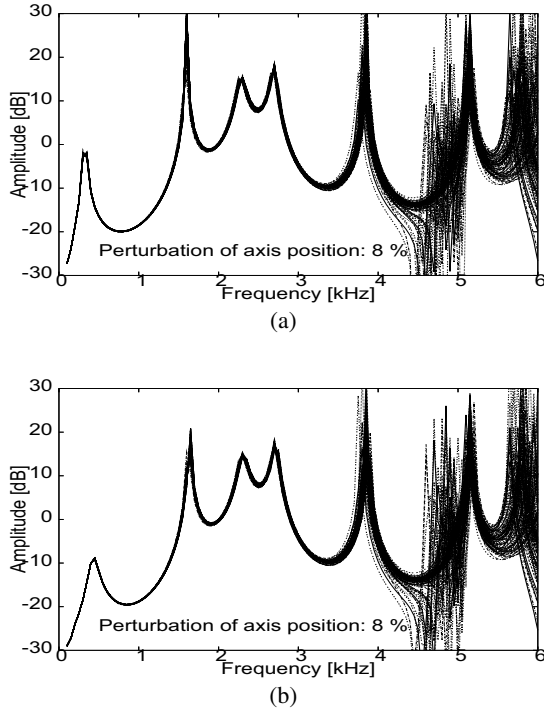


Figure 7: Transfer characteristics of asymmetric 36 section configuration with random perturbation of axis positions. 100 models with 8% perturbation. (a) rigid wall (b)  $Z_w = 1900 + j\omega 1.2[g/(cm^2 \cdot s)]$ .

propagative higher-order modes, and are almost the same as the peaks in rigid wall condition. It can be said that even though the attenuation of the higher-order modes is larger than that of plane waves, the wall can be regarded as rigid enough for this value of the wall impedance.

### 3.2.2. Asymmetric multiple section

To imitate a small change of the vocal-tract shape, the axis position  $(x_i, y_i)$  of the  $i$ -th section is modified while the area of that section is kept unchanged.

$$\begin{aligned} x_i &= x_{i,0} + \varepsilon L_{x,i} R[-1, 1] \\ y_i &= y_{i,0} + \varepsilon L_{y,i} R[-1, 1] \end{aligned} \quad (16)$$

where  $L_{x,i}$  and  $L_{y,i}$  are the dimensions of the  $i$ -th section, and  $R[-1, 1]$  a uniform random number between -1 and 1.  $\varepsilon$  is a parameter to specify the maximum perturbation of the axis position. Figure 7 shows the transfer characteristics of 36-section configuration given in figure 1, with changing the axis position of each tube. 100 models having slightly different shapes have been made with  $\varepsilon = 0.08$ .

It is clearly seen that lower peaks are stable even small change in shape is given. The transfer characteristics above 4 kHz are largely influenced by the small change of the axis position with the appearance of sharp peaks and zeros. Compared with the rigid wall condition, an increase of bandwidth and upward shift of the first peak are also seen. The characteristics in higher frequencies, however, are similar indicating the less sensitivity to the values of the wall impedance.

## 4. Conclusions

The wall impedance of the vocal-tract was introduced in the computation of the propagation constant of the higher-order modes. The frequency characteristics of both the attenuation and phase constants, and the transfer impedance were presented. The results showed an increase of bandwidth and a slight upward shift of peaks especially in lower frequencies while the sharp peaks in higher frequencies were less sensitive to the wall impedance.

Other internal loss factors, such as air properties (viscosity and heat conductivity) or radiation from the skin should be further investigated for the improvement of the three-dimensional analysis of the realistic vocal-tract.

## 5. Acknowledgements

The author would like to thank Dr. Hiroki Matsuzaki for valuable discussion on acoustic analysis of vocal-tract. Part of this work has been supported by a research project of High-Tech Research Center, Hokkai-Gakuen University.

## 6. References

- [1] Matsuzaki,H. and Motoki,K., "Study of acoustic characteristics of vocal tract with nasal cavity during phonation of Japanese /a/", *Acoust. Sci. & Tech.*, **28**,2,124-127, 2007.
- [2] Matsuzaki,H., Serrurier,A., Badin,P. and Motoki,K., "3D and plane wave acoustic propagation comparison for a Japanese and a French vowel /a/ with nasal coupling", *Proc. Autumn meeting Acoust. Soc. Jpn*, 2-4-15, 471-474(2007).
- [3] Motoki,K., Pelorson,X., Badin,P. and Matsuzaki,H. "Computation of 3-D vocal tract acoustics based on mode-matching technique", *Proc. ICSLP2000, Beijing*, 461-464, 2000.
- [4] Motoki,K. and Matsuzaki,H., "Computation of the acoustic characteristics of vocal-tract models with geometrical perturbation", *Proc. ICSLP2004 (INTER\_SPEECH2004-ICSLP)*, Jeju, TuB602p.16, 521-524, 2004.
- [5] Morse,P.M. and Ingard,K.U., *Theoretical Acoustics*,Chap.9, McGraw-Hill,1968.
- [6] Crocker,M.J., *ed.*, *Handbook of acoustics*, Chap.7, Wiley, 1998.
- [7] Flanagan,J.L., *Speech Analysis Synthesis and Perception*, 2nd ed.,p.68, Springer-Verlag, 1972.
- [8] Ishizaka,K., French,J. and Flanagan,J.L. "Direct determination of vocal tract wall impedance", *IEEE Trans. Acoust. Speech and Signal Proc.*, **ASSP-23**,4,370-373, 1975.
- [9] Suzuki,J., "Discussions on vocal tract wall impedance", *J. Acoust. Soc. Jpn*, **34**,3, 149-156, 1978.
- [10] Lunde,P., "Acoustic transmission-line analysis of formants in hyperbaric Helium speech", *Proc. IEEE Int. Conf. on ICASSP'85*, 3, 1141- 1144, 1985.
- [11] Kamiyama,N., Miki,N. and Nagai,N., "Measurement of acoustic reflection characteristics of the human cheek", *J. Acoust. Soc. Jpn (E)*, **11**,4, 207-214, 1990.
- [12] Dang,J., Nakai,T. and Suzuki,H., "Measurement of cheek impedance by sound pressure in oral cavity and acceleration of vibrating cheek", *J. Acoust. Soc. Jpn*, **48**,9, 621-628, 1992.